Catalytic nanocapillary condensation and epitaxial GaN nanorod growth

H. W. Seo* and Q. Y. Chen[†]

Department of Physics and Texas Center for Superconductivity and Advanced Materials, University of Houston, Houston, Texas 77204-5002, USA

L. W. Tu and C. L. Hsiao

Department of Physics and Center for Nanoscience and Nanotechnology, National Sun Yat-Sen University, Kaohsiung, Taiwan 80424, Republic of China

M. N. Iliev and W. K. Chu

Department of Physics and Texas Center for Superconductivity and Advanced Materials, University of Houston, Houston, Texas 77204-5002, USA

(Received 14 March 2005; published 13 June 2005)

Intrinsic catalytic process by capillary condensation of Ga atoms into nanotrenches, formed among imping-ing islands during the wurzite-GaN thin film deposition, is shown to be an effective path to growing GaN nanorods without metal catalysts. The nanocapillary brings within it a huge imbalance in equilibrium partial pressure of Ga relative to the growth ambient. GaN nanorods thus always grow out of a holding nanotrench and conform to the boundaries of surrounding islands. The nanorods are epitaxially oriented with $\langle 0001 \rangle_{GaN} \| \langle 111 \rangle_{Si}$ and $\langle 21\bar{1}0 \rangle_{GaN} \| \langle 110 \rangle_{Si}$ similar to the matrix. Concaved geometry is essential and is a condition that limits the axial dimension of the nanorods protruding above the base (matrix) material region. Revelation of the growth mechanism in the current context suggests that fabrication of nanoquantum structures with controlled patterns is enabling for any attainable dimensions.

PACS number(s): 81.07.Vb, 81.15.Aa

GaN has undergone extensive research and development for the past decade because of its perceived commercial value for blue laser and light emitting diode applications.[1,2] In these efforts, one of the main challenges was to obtain morphologically smooth thin films, since samples frequently ended in rough surface or columnar structures, which are undesirable defects from a two-dimensional thin film device application perspective. More recently, however, such spuri-ous structures have attracted a great deal of interest, as many believe they may be exploited for controlled formation of nanostructures suitable for quantum device purposes.[3] In-deed, plenty of alluring nanogeometric shapes have been re-ported, ranging from flexible and often free-standing or en-tangled nanowires[4–6] to epitaxial spikes of nanorods or nanocolumns standing on a base material.[7–10] Such attempts in nanostructure formation, nonetheless, must move from the presently naturally occurring processes to scalable designs such as patterned arrays in order to realize their full applica-tion potentials. For this purpose, it would be desirable to understand the mechanism of nanostructure formation from which some process design rules may be inferred.

Previous studies on the growth mechanisms of nanowires of GaN[5] and other semiconductors[7,11] all more or less rested on the classical catalyst-assisted vapor-liquid-solid (VLS) or vapor-solid (VS) models, established earlier in an effort to understand the growth of whiskers.[12] The nanorods observed in this work, nevertheless, are quite different in that they are always accompanied by nanotrenches[13–15] and require no ex-trinsic metallic catalysts as the nuclei. These phenomena, we believe, stem from a nanocapillary condensation of Ga at-oms. Capillary condensation is a well-known phenomenon, as now commonly documented in many textbooks on physi-

cal chemistry of surfaces. A recent review article by Elliott has discussed it in great detail, citing many classic references as well as pointing out some of their errors.[16] Nanocapillary condensation has never been considered as associated with the growth of nanorods while many have studied and under-stood the formation of nanorods in the contexts of VLS and VS mechanism.[9,10] We illustrate in this work that the capil-lary condensation of Ga atoms into the nanotrenches serves as a catalytic agent in lieu of the traditionally used metallic nanocatalysts, to trigger the nanorod growth.

The objective of this work is to elucidate this point of view by modeling the growth mechanism based on the ob-served nanorods in relation to their nanotrench precursors. Our interest in this study was mainly on the wurtzite struc-ture (0001) GaN epitaxial films populated with nanorods. Underneath such samples typically is a template buffer layer deposited at a lower temperature (500–600 °C) under high nitrogen to gallium ratio conditions. The GaN films were grown by plasma assisted molecular beam epitaxy (MBE) on $\langle 111 \rangle$ oriented silicon substrates, as reported earlier.[17] The nanorods, with lateral dimensions $\sim$10–100 nm and longi-tudinal dimensions $\sim$0.4–0.6 μm above the film surface, al-ways coexist with a "nanoflower" pattern.[17] They are largely rooted near the homoepitaxial buffer layer Si alongside the nanotrench, as shown in Fig. 1. The nanoflower is essentially a V-shaped crater of sixfold symmetry, with its bottom con-nected to a trench which extends through the entire film down to the silicon interface. Similar geometry on the close packed planes of some other materials of either cubic symmetry,[18] or wurtzite structure, such as SiC,[19] have also been observed. The nanorods are pin shaped, by and large, with tip pointed toward the bottom, and are detached from
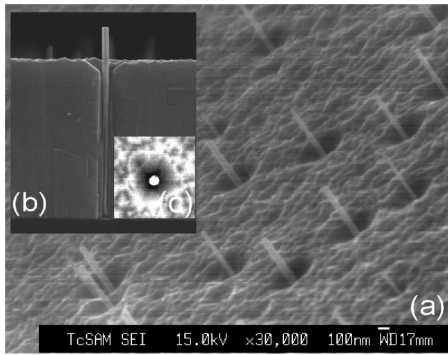
FIG. 1. SEM picture of GaN nanorods. (a) GaN nanorods protruding out of nanoflower craters (20° tilt view). (b) Cross-sectional view. (c) Top view.

the walls of the nanotrenches typically by a lateral gap of several nanometers. These nanorods, nanotrenches, and their accompanying nanoflowers are randomly dispersed, sometimes clustering around different regions of the sample.

The origin of nanotrench formation has hitherto mostly been attributed in literature to the threading dislocation, as suggested by Frank.[20] In this context, a dislocation of a large Burgers vector may lower its energy by emptying the highly strained core region. In balance, the critical core radius is $r = Gb^2/8\pi^2\gamma$, where G is the shear modulus, b is the Burgers vector, and γ is the surface energy of the material. (Here the planes of relevance are the $\{10\underline{1}0\}$ family.) Unfortunately, the observed core radii ($2r \sim 10$–100 nm) are too large per core energy.[13–15] Suppose that b is along $\langle 0001 \rangle$ and $b = 0.518$ nm (the lattice constant along the c axis), $G = C_{13} \sim 10^{11}$ N/m^2,[2] and $\gamma \sim 1.89$ J/m^2,[21] then we have $2r \sim 0.34$ nm, suggesting that the existence of such open cores is not driven by the strain-field of a dislocation, otherwise this would have given $\gamma \sim 0.006$ J/m^2, which is out of range by far for a solid compound.

In order to account for the above mentioned discrepancy, we suggest that there are two types of nanotrenches. Type I trench, having smaller diameter (~ 1 nm) and containing no nanorods, can indeed be the trace of an open-core dislocation[22] situated at the center of an island. Type II trench, as referred to in this paper simply as the nanotrench, on the other hand, is typically one hundred times larger. Earlier reports showed that this type of trench could either be empty,[13,15] or filled with inversion domains.[14,15] Within this work, however, we realize that the type II nanotrenches come to exist as a result of coarsening hexagonal islands. One may ask why it would favor island growth that leads to the nanotrenches in lieu of a smooth film since, in classical views,[23] lattice mismatch strain are relieved beyond a critical thickness through the generation of misfit dislocations. The answer lies in the recent recognition that strain relief can also occur instead by way of surface roughening,[24] as demonstrated in single layer thin films or superlattices of group IV compounds[25] and III–V compounds.[26] Surface roughening relaxes mismatch strain at the cost of higher total surface energy, giving a thermodynamically lower energy state as compared to that of a smooth, strained, and possibly concaved surface. This roughened surface is a precursor to is-
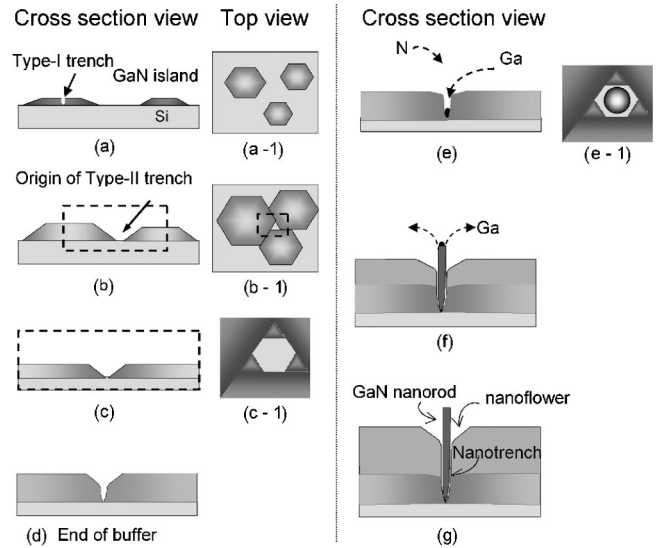
FIG. 2. Evolution of nanotrench and nanorod: (a) Initial stage of GaN island growth containing type-I trenches. (b) Impinging hexagonal islands and the formation of a triangular void region. (c) Corner filling of the triangular void and its evolution into hexagonal shape, precursor to the nanoflower. (d) Evolution of the nanoflower and start of the nanotrench formation. (e) Capillary condensation of Ga atoms in the trench. (f) VLS growth mechanism prevails and the nanorod grows faster, leading to protrusion above the nanoflower. As the protrusion occurs, the condition for capillary condensation diminishes and VS growth mechanism takes over. (g) The ultimate structure.

land or columnar structure. In the end the strain field would be unevenly distributed and the trough regions of the roughened surface should be more strained than their crest counterparts. This is in agreement with our earlier observations at the GaN buffer to substrate interface.[17] For GaN on AlN, it is known that the lattice mismatch $\delta = (a_{GaN} - a_{AlN})/a_{AlN}$ is $\sim +2.4\%$ and the critical thickness, beyond which surface roughening takes place, is only 1–3 monolayers.[26] Hence, island formation for GaN on Si in our samples should start even earlier at the interface region since there $\delta = (a_{GaN} - a_{Si})/a_{Si} \sim -17\%$. This unusually large lattice mismatch might have been reconciled to a larger coincidence lattice with respect to the Si substrate, though this hypothesis remains to be verified.

The nucleation and growth process, we reckon, start with three randomly chosen precursor nuclei on the vertices of an irregular triangle [Fig. 2(a)]. Consequently, a voided region of equilateral triangle would develop as illustrated in Fig. 2(b-1) when the islands encounter each other. Certainly, on some occasions, the islands may leave no voided regions behind if the relative positions of the nuclei happen to be along $[1\underline{1}0]_{Si}$ or $[2\underline{1}\underline{1}0]_{GaN}$ directions. But in any case, in the simplest scenario, the voided triangular areas are thermodynamically unstable, unlike islands of metallic elements for which triangular form is common.[27] For growth that occurs on the close-packed $\{111\}$ plane of a Si lattice, we hence suggest that a transformation would take place to reduce the surface energy by corner filling via some self-regulated surface diffusion along the edges where the islands wet the sub-

strate. This eventually results in a hexagonal nanotrench, as sketched in Fig. 2(c-1). Such concept was vaguely touched upon by Elsner et al.[28]

With the hexagonal empty region in place, the islands would continue to grow in the vertical dimension and the six facets surrounding the region would then be elevated, eventually becoming what one observes as a six-leaf nanoflower. The nanotrenches underneath the nanoflower are essentially like an attached capillary tube [Fig. 2(d)]. When the capillary tube is long enough, plausibly at the end of low temperature buffer layer growth when the aspect ratio of the tube is high, capillary condensation of Ga atoms occurs as a consequence of the decreases in the equilibrium vapor pressure due to the reduced radius of curvature of a concave surface, as seen from the Thomson (Lord Kelvin) equation $k_B T \log[P_{Ga}(r)/P_{Ga}(\infty)] \sim -2\gamma^{LV} V_{Ga}/r$.[16] For a convex surface, conversely, the negative sign is reversed and a small radius of curvature would favor evaporation. Whether the governing equation remains valid at nanoscales is an unsettled question, but by assuming that it does, then, as a cross examination, for 100 nm, 1, and 10 μm tubes, the ratio $P(r)/P(\infty)$ are, respectively, $\sim 5 \times 10^{-24}$, 5×10^{-3} and 0.6 with molar volume for Ga being ~ 11.8 cm^3/mol. The flat surface equilibrium partial pressure is $P_{Ga}(\infty) \sim 10^{-8}$ Torr at 500–600 °C for the buffer layer and $\sim 10^{-5}$ Torr at 720 °C for the ultimate film.

GaN nanorod grows faster along $\langle 0001 \rangle$ via the canonical VLS mechanism[12] by reaction of the nitrogen plasma with the Ga condensates while their surrounding GaN islands also grow alongside to form the base materials, though at a slower rate. Figures 2(c)–2(g) illustrate this sequence of evolution. The cross-sectional views indicate that the lateral dimensions of nanorods and nanotrenches are graded in the beginning and there is a gap in-between, as shown in Figs. 2(d)–2(f). Here, we show when capillary condensation starts and nanorod eventually sprouts from the nanotrench due to its higher growth rate. As the nanorod outgrows the nanotrench and starts to stick out of the base film surface, an intermediate case between Figs. 2(e) and 2(f), the equilibrium vapor pressure would gradually increase which favors the evaporation of the droplets on top of the nanorod [Fig. 2(f)]. The process eventually reaches a steady state after which the rods grow at the same rate as the surrounding film via VS growth mechanism since the conditions for capillary condensation no longer exist; otherwise the nanorods would grow enormously long and thus stand far above the base material, which is not what was observed, as suggested in Fig. 2(g). According to our observation, as indicated by the top views in Figs. 3(a)–3(c), where the scanning electron microscopy (SEM) surface morphologies of three samples are shown, at the beginning stages of island formation and impingements, i.e., for the buffer layer, only nanotrenches but no nanorods exist. As higher temperature growth commences, nanorods begin to emerge as seen in Fig. 3(b). This coincides with the above reasoning that capillary condensation does not occur until the nanotrench is deep enough to foster the process. Moreover, the size of a nanorod depends on that of the holding nanotrench, while that of the nanotrench, in turn, depends on the density of the impinging islands with relevant lateral dimensions (also on order of
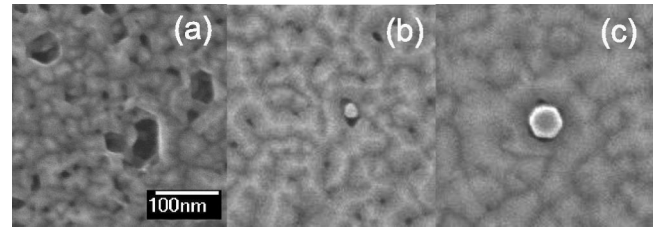
FIG. 3. Surface morphologies showing various stages of nanorod formation: (a) buffer layer 37 nm grown at 590 °C, (b) 50 nm film at 720 °C on buffer layer (a), and (c) 150 nm film at 720 °C on buffer layer (a).

10–100 nm). As seen from the evolving morphology, both nanorod and matrix islands coarsen with time at a constant temperature as seen by comparing Figs. 3(c) with 3(b). We observed from the top-view SEM micrographs (Fig. 3) that the nanorods would grow larger as the matrix grows thicker until it reaches an optimal size and then remains constant. Here, as the film grows thicker or if it grows at higher temperatures, the extent to which strain relief occurs also expands until the island growth and strain relaxation run their courses. At that moment, the moundlike islands would finally take shape. The slant of these islands, and hence, the ultimate sizes of the nanotrenches they enclose, is a manifestation of the lattice mismatch between GaN and its Si substrate at the film growing temperature. Beyond that point the relaxation process is complete and the sizes of nanorods would stop growing.

The nanorod density also depends on the growth temperature, though in a more complex way than simply being proportional to the island density. For instance, direct growth without low-temperature buffer layer would foster columnar structure and suppress nanorod growth, which is consistent with the concept of nanocapillary condensation because, at high temperature, there are less regions of coalescence where the radius of curvature is small enough—most are flat boundaries formed by impinged nanocolumns or submicron columns. Sporadic nanorods are observable at those corner sites where the radius of curvature meets the criterion of nanocapillary condensation.[29] This suggests that while the matrix most likely would follow the traditional thermal mechanism of grain or island growth (including columnar structures), nanorod growth is highly restricted by the seeding of Ga atoms in the nanocapillary. Furthermore, the shape of nanorod conforms to that of the holding nanotrench and can, in reality, be less symmetric than a perfect hexagon depicted above. As shown in the four SEM micrographs of Fig. 4, we see some intermediate states of a geometrical evolution of the nanorods. These geometrical variants may be related to the asymmetric corner filling of the triangular basins, as alluded to earlier, at the beginning of nanotrench formation, thus also further providing a convincing evidence for the conformity of nanorods to their holding nanotrenches.

Note other factors such as the Ga:N ratio and the method of film growth can also play an intricate role on the nanostructure formation. Lower temperature deposition under N-rich condition favors higher nucleation density[22] while slower growth rates give more time for condensation and
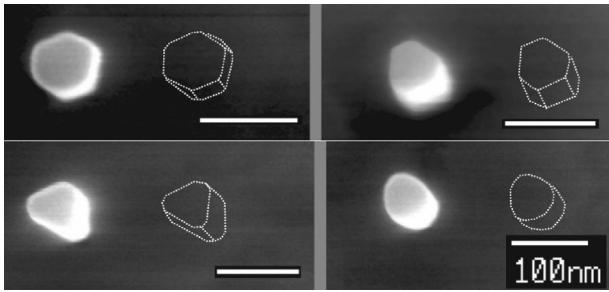
FIG. 4. SEM top view micrographs showing different geometric shapes assumed by the nanorods, manifesting the intermediate stages of corner filling mentioned in the text.

FIG. 5. SEM micrographs of GaN nanostructures before (left) and after (right) H_3PO_4 etching. The base area is Ga polar for its resistance to the etching while the nanorods are likely to be N polar for their dissolution by the H_3PO_4.

nitrogen atom diffusion in the droplet. In this vein, it may be understandable why no nanorod formation has been observed so far for other methods of inherently higher growth rate operating at much higher temperature such as metalorganic chemical vapor deposition (MOCVD). Certainly, this warrants a more careful investigation, even though plasma-assisted MBE growth at medium temperatures of 750–800 °C truly appears to be most favorable for the GaN nanorods to form[8–10,17] as long as the growth starts with a low temperature deposited N-rich buffer layer. The nanorods are epitaxially orientated, based on electron backscatter Kikuchi patterns, with rod axis//$\langle 0001 \rangle$ of the base area and $\langle 111 \rangle_{Si}$ while the closed packed $\langle 2\overline{1}\overline{1}0 \rangle$ axis for both the nanorods, nanotrenches and the base film regions are all parallel to the $\langle 110 \rangle$ close packed direction of the {111} oriented silicon substrate.[30] Such high degree of epitaxy implies the existence of molecular interacting forces strong enough to dictate atomic arrangements of the nanorods with respect to their surrounding matrix. The matrix is Ga polar, judged from its resistance to H_3PO_4 etching as compared to the nanorods,[31] which all disappeared after etching, as shown in Fig. 5 where the SEM micrographs of surface morphology before and after etching are compared. However, due to the flimsiness of nanorods as bound by nanotrenches, we cannot

conclude with certainty that the nanorods are N-polar. We take this cautious note because it is possible that as the surrounding nanotrenches are widened by etching, the nanorods might have lost their mechanical support and be washed away by the etching solution.

In summary, we report that nanotrenches catalyze the formations of GaN nanorods through the capillary condensation of Ga atoms in an ultrahigh vacuum based plasma-assisted MBE system. This implies that self-assembled extrinsic metal catalysis, frequently used to produce nanowires and nanorods, can be replaced with nanocapillaries. The capillaries reported here are the nanotrenches which arise from impinging islands during the film growth. The concept of nanocapillary condensation is inspiring as it can be extended to integrated fabrications of designed patterns for useful electron or photonic devices with the help of contemporary advanced lithographic means.

---

*Electronic address: hseo@uh.edu

†Author to whom correspondence should be addressed. Electronic address: qchen@uh.edu

[1] F. A. Ponce and D. P. Bour, Nature (London) **386**, 351 (1997); J. W. Orton and C. T. Foxon, Rep. Prog. Phys. **61**, 1 (1998); O. Ambacher, J. Phys. D **31**, 2653 (1998); S. J. Pearton, J. C. Zolper, R. J. Shul, and F. Ren, J. Appl. Phys. **86**, 1 (1999).

[2] H. Morkoc, *Nitride Semiconductors and Devices* (Springer, New York, 1999); J. H. Edgar, Samuel Strite, Isamu Akasaki, Hiroshi Amano, and Christian Wetzel, *Properties, Processing and Applications of Gallium Nitride and Related Semiconductors* (INSPEC, London, 1999).

[3] V. A. Shchukin, N. N. Ledentsov, and D. Bimberg, *Epitaxy of Nanostructures* (Springer, New York, 2003).

[4] Justin C. Johnson, Heon-Jin Choi, Kelly P. Knutsen, Richard D. Schaller, Peidong Yang, and Richard J. Saykally, Nat. Mater. **1**, 106 (2002).

[5] W. Han and A. Zettl, Appl. Phys. Lett. **80**, 303 (2002); W. Han, S. Fan, Q. Li, and Y. Hu, Science **277**, 1287 (1997).

[6] L. X. Zhao, G. W. Meng, X. S. Peng, X. Y. Zhang, and L. D. Zhang, J. Cryst. Growth **235**, 124 (2002).

[7] H. T. Ng, J. Li, M. K. Smith, Pho Nguyen, A. Cassell, and M. Meyyappan, Science **300**, 1249 (2003).

[8] M. Yoshizawa, A. Kikuchi, M. Mori, N. Fujita, and K. Kishino, Jpn. J. Appl. Phys., Part 2 **36**, L459 (1997).

[9] R. Birkhahn and A. J. Steckl, Appl. Phys. Lett. **73**, 2143 (1998).

[10] E. Calleja, M. A. Sanchez-Garcia, F. J. Sanchez, F. Calle, F. B. Naranjo, E. Munoz, U. Jahn, and K. Ploog, Phys. Rev. B **62**, 16826 (2000).

[11] A. M. Morales and C. M. Lieber, Science **279**, 208 (1998).

[12] A. P. Levitt, *Whisker Technology* (Wiley-Interscience, New York, 1970).

[13] W. Qian, G. S. Rohrer, M. Skowronski, K. Doverspike, L. B. Rowland, and D. K. Gaskill, Appl. Phys. Lett. **67**, 2284 (1995).

[14] F. A. Ponce, W. T. Young, D. Cherns, J. W. Steeds, and S. Nakamura, Mater. Res. Soc. Symp. Proc. **449**, 405 (1997).

[15] Z. Liliental-Weber, Y. Chen, S. Ruvimov, and J. Washburn, Phys. Rev. Lett. **79**, 2835 (1997); Z. Liliental-Weber, Y. Chen, S. Ruvimov, W. Swider, and J. Washburn, Mater. Res. Soc. Symp. Proc. **449**, 417 (1997). Note: "trench" has been adopted here following the microelectronic processing industry convention where it represents an isolated pit-shaped or well-shaped region more than a conventional trench which implicates a continuous extension of such a region.

[16] J. A. W. Elliott, Chem. Eng. Educ. **35**, 274 (2001), and the references cited therein.

[17] L. W. Tu, C. L. Hsiao, T. W. Chi, I. Lo, and K. Y. Hsieh, Appl. Phys. Lett. **82**, 1601 (2003).

[18] S. Takasu and S. Shimanuki, J. Cryst. Growth **24/25**, 641 (1974).

[19] H. Hobgood, D. L. Barrett, J. P. Mchugh, R. C. Clarke, S. Sriram, A. A. Burk, J. Greggi, C. D. Brandt, R. H. Hopkins, and W. J. Choyke, J. Cryst. Growth **137**, 181 (1994).

[20] F. C. Frank, Acta Crystallogr. **4**, 497 (1951).

[21] J. E. Northrup and J. Neugebauer, Phys. Rev. B **53**, R10477 (1996).

[22] C. Kruse, S. Einfeldt, T. Bottcher, and D. Hommel, Appl. Phys. Lett. **79**, 3425 (2001).

[23] J. W. Mathews and A. E. Blakeslee, J. Cryst. Growth **27**, 118 (1974); J. W. Mathews, J. Vac. Sci. Technol. **12**, 126 (1975).

[24] B. J. Spencer and J. Tersoff, Phys. Rev. Lett. **79**, 4858 (1997).

[25] D. E. Jesson, S. J. Pennycook, J. M. Baribeau, and D. C. Houghton, Phys. Rev. Lett. **71**, 1744 (1993); H. Gao and W. D. Nix, Annu. Rev. Mater. Sci. **29**, 173 (1999).

[26] C. Adelmann, N. Gogneau, E. Sarigiannidou, J. L. Rouvière, and B. Daudin, Appl. Phys. Lett. **81**, 3064 (2002).

[27] Jing Wu, E. G. Wang, K. Varga, B. G. Liu, S. T. Pantelides, and Zhenyu Zhang, Phys. Rev. Lett. **89**, 146103 (2002).

[28] Joachim Elsner, Alexander Th. Blumenau, Thomas Frauenheim, Robert Jones, and Malcolm I. Heggie, MRS Internet J. Nitride Semicond. Res. **5S1**, W9.3 (2000); url: http://nsr.mij.mrs.org/5S1/W9.3/article.pdf

[29] C. L. Hsiao, Ph.D. thesis, National Sun Yet-Sen University, Taiwan, Republic of China, 2004.

[30] H. W. Seo, Q. Y. Chen, M. N. Iliev, W. K. Chu, L. W. Tu, C. L. Hsiao, and James K. Meen, cond-mat/0503195 (unpublished).

[31] D. Huang, P. Visconti, K. M. Jones, M. A. Reshchikov, F. Yun, A. A. Baski, T. King, and H. Morkoç, Appl. Phys. Lett. **78**, 4145 (2001).